International Journal on Advanced Science Engineering Information Technology

Vol.11 (2021) No. 2
ISSN: 2088-5334

# Characterization of River Sediments in Loja-Ecuador

Gabriela Carolina Andrade Lescano[a,*], Alex Mauricio Matheus Mayorga[b], Javier Martìnez-Gomez[c]

[a] *Instituto de Investigación Geológico y Energético (IIGE), Quito, Ecuador*
[b] *Universidad Central del Ecuador Quito, Ecuador*
[c] *Universidad International SEK, Quito Albert Einstein s/n and 5th, Ecuador*
*Corresponding author: *gabriela.andrade@geoenergia.gob.ec*

***Abstract*—This research's main objective is to delineate areas with a high concentration of "pollutant" elements that imply a risk for the ecosystem and inhabitants' health in the Cordillera Real, south of Ecuador. To this end, a survey was carried out applying statistical analysis of the data. Specifically, the method of ordinary Kriging and Lepeltier is used to sort the data in populations according to their concentration. Previously, the information was compared with national (TULAS) and international regulations (Environmental Canada). These metals' spatial distribution is shown in concentration maps for each element (Hg, Pb, Zn, As, and Cu), where the potential villages exposed to these anomalies are displayed. In this sense, the samples' chemical digestion was conducted to quantify the atomic emission technique's before-mentioned pollutants' concentration. It was also correlated with geology, mineral occurrences, and metallogeny evidence to conclude that Pb and Zn anomalies are related to San Lucas granodiorite's intrusion, whereas Cu and Hg with local mineralization of sulfides, and as may be with domestic and industrial discharges. Finally, even though the anomalous concentrations of metallic elements were found to be characteristic of the lithology, cautions should be taken to safeguard the health of people and agriculture because there is evidence of elements such as As and Hg bioaccumulation in species that are part of the food chain.**

***Keywords*— Anomaly; bioaccumulation; Lepeltier; Kriging; correlation; geology; watershed; mineralization; pollutant.**

*Manuscript received 8 Nov. 2020; revised 12 Jan. 2021; accepted 7 Feb. 2021. Date of publication 30 Apr. 2021.*


## I. INTRODUCTION

The National Geological Cartography Programs are intended to show previous and updated geological information. In the same way, they include information about morphology associated with mass movements and identification of places with potential geological interest and geological heritage interest. Into the decade of seventies, the National Geological Cartography Program developed the geological survey in Loja, applying a 1: 100000 scale in which the Zamora Group metamorphic units and sedimentary sequences of the Loja Basin are located. Trouw makes a cut from Saraguro to Zamora [1]. Here, the groups of metamorphic rocks in the Cordillera Real, San Lucas, and Sabanilla are clustered. In 1986, the Cordillera Real project was developed in which the cartography of the mountain range was executed based on numerous geotargets described in annual technical reports and their respective cartography. Also, detailed geology, which defines different lithotectonic terrains and regional structures has been studied [2]. This work published the geological map of the Cordillera Real at a scale of 1: 500,000.

As part of the same project, regional geochemistry was carried out in the mountains to define mineral clues. In this sense, in the northeast corner of the area under study, they determined the occurrence of anomalies of W, Sn, and Cr [3]. Besides, the basin's geodynamic study was carried out from the survey of stratigraphic sequences and the structural analysis [4]. Subsequently, they studied the intra-mountainous basins of southern Ecuador, including Loja, to present a general map with details of the stratigraphy and sedimentology in different units. The main contribution was dating with fission traces and paleontology, which established an evolution model for the Loja basin [5]. In recent years, ground movements along the Loja-Zamora road were characterized, mentioning that its susceptibility is related to the metamorphic rocks of the Chigüinda, and Sabanilla units [6].

However, previous research has not carried out an analysis of this area's river sediments yet. This analysis will quantify the sediments' chemical levels, their toxicity, and potential

pollution impacts on local communities [7]. In this paper, samples of river sediments have been taken in the Loja Norte topographic sheet's channels. It is necessary to analyze this data to define anomalies (high concentrations) of elements detrimental to inhabitants' health and consumption crops [8-10]. For this, the geochemical data of Hg, As, Cu, Zn, and Pb will be geostatistical processed to determine potentially toxic concentrations as well as their background and geochemical threshold. In regional geochemical surveys, spatial distribution maps are commonly used to give detailed information and detect if their potential sources are anthropogenic or geogenic [11]. Besides, geochemical maps' elaboration contributes to obtaining sparse patterns in places without accessible information by interpolating data. In particular, some tools allow avoiding the preprocessing of data, such as kriging [12], [13]. Moreover, sediments' ability to absorb organic and inorganic pollution becomes this kind of study is an important tool for monitoring water quality and heavy metals mobility [14].

It is important to compare the results with national regulations (TULAS) and international regulations (Environmental Canada). Besides, they must be correlated with geology, metallic signs, and hydrographic basins to define possible natural sources of these elements. Thus, the current research can be used as an environmental baseline for future projects in this sector [15].

## II. Material and Method

The analysis of the river sediments was carried out in laboratories for 35 elements, of which six (Hg, As, Cu, Zn, Cd, and Pb) were initially considered for their respective geostatistical analysis interpretation. Nevertheless, Cd was removed from the study because its concentrations were lower than the measurement equipment's limits. The total of samples collected in the field and considered for the study were 224. These samples were distributed throughout the entire extension of the Loja Norte topographic sheet (Figure 1).

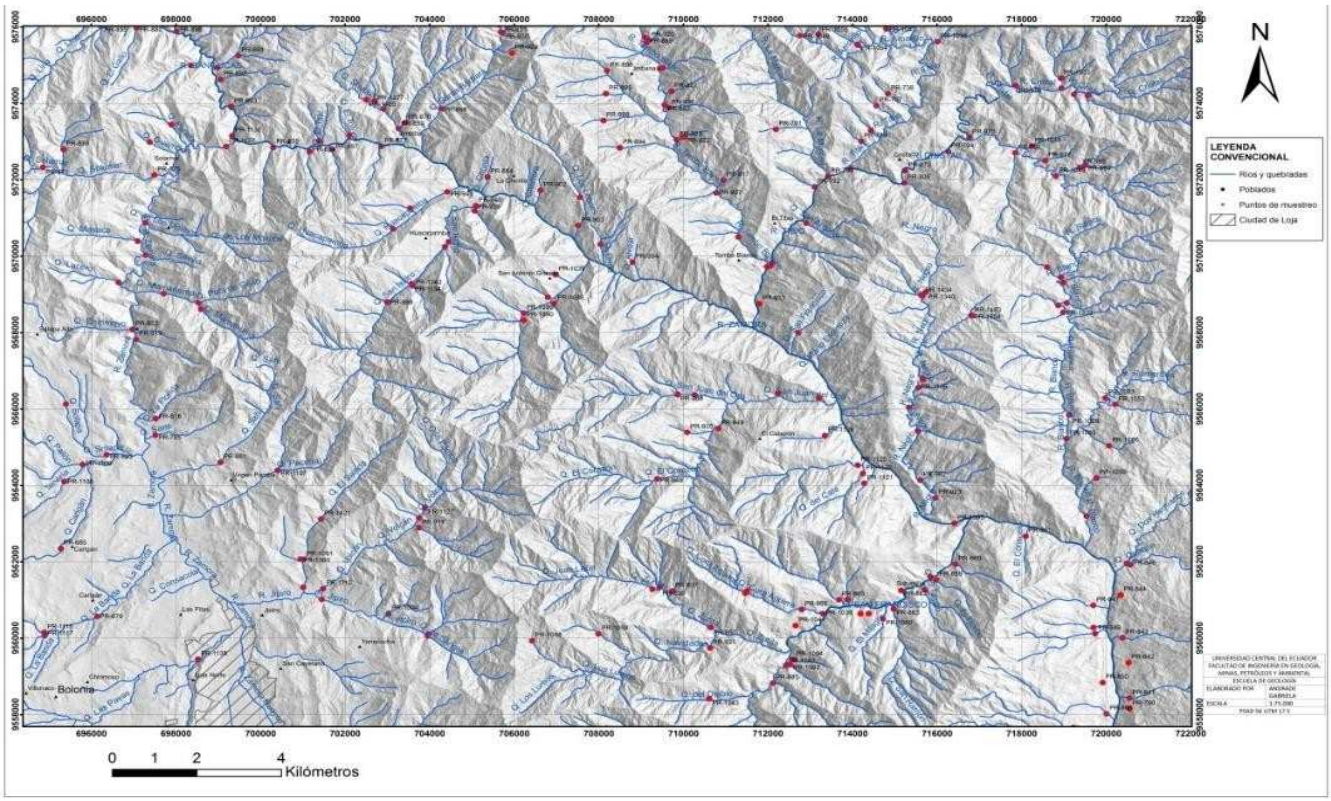


Fig. 1 Map of sample locations in the area under study

### A. Sediment Sampling

Samples were taken from 20 to 50 m upstream from each drain's confluence to avoid contamination by flood zones. Additionally, samples were taken at the river's low energy zone, where sediments are accumulated [16]. Applied instruments must be clean to avoid contamination in the samples. The first plastic pan is placed in a balanced way to avoid spillage of the sample. Over a tray, a 2 mm mesh sieve is placed. They are located between 3 and 4 points in the tributary where the water's erosive power is low. A sufficient sample is collected from the located points using a small shovel, and 250 g of fluvial sediment is sent for laboratory analysis. A recommendation in this process, it is necessary to use and fill three pots of material. Two sample shovels are placed at the same time on the 2 mm mesh sieve. Then, the sample is washed by handmade firm circular movements and using up to 3 liters of water taken from the same channel and recycling it. Then, the excess is shaken horizontally and vertically before being discarded. This process is carried out until the plastic tray under the 2mm mesh is full. The second plastic tray, in which the 80-mesh sieve is placed, is balanced. Two shovels are placed at the same time that the sample is accumulated in the plastic tray.

Similarly, the sample is washed by handmade circular movements. Firmly, but without pressing too much since this

80-mesh sieve is very delicate, it uses three litters of the tributary water for the entire process and then recycles it from the plastic tray. All the material that does not pass the 80 mesh is coarse sediment, and it is placed in the two metal pans. On the other hand, the material that passes the mesh is the river sediment. This process is carried out until the entire sample has been washed from the first plastic tray. The second plastic tray with the fluvial sediment is left, resting at an angle for 30 min for settling the sample correctly. The two metal troughs containing the coarse sediment are washed with elliptical movements until all that remains in the troughs is the heavy sediment. The heavy sediment and the fluvial one is stored in hermetic covers with their respective codification for their later analysis. The covers are placed in a plastic container and left to dry at room temperature. While the filtering is resting, some data such as GPS coordinates, map coordinates, water quality, environment, conditions, and drainage status are taken, photography, sediment color, contamination, flow type, time, etc. Finally, these samples are analyzed in the laboratory, and the results are interpreted.

### *B. Chemical analysis of river sediments*

For the chemical analysis of fluvial sediments, chemical digestion is applied using the humid acid solution, using a Milestone brand microwave model Ethos One. The quantification is performed applying the atomic emission technique with an ICP-OES equipment, brand Perkin Elmer, model Optima 8 300 that is capable of quantifying a wide variety of elements in the periodic table using short periods, and it has low instrumental detection limits, the value of which depends on the element under analysis [17].

### *C. Statistical Analysis of River Sediment Data*

Before statistical analysis, geochemical data must be carefully screened to account for missing values (unreported, usually appear as blank or NULL when received from the laboratory) and censored values (greater or less than the detection limits (DLs). These two types of data cannot be used for numerical processing or statistical studies, but they do not affect process recognition results [18].

To carry out the AEDE, descriptive statistical tools are used, such as the construction of frequency tables, calculation of statistical measures of central tendency (mean, median, and mode), non-central position measures (quartiles, percentiles, deciles), measures of dispersion (standard deviation, variance, and coefficient of variation), and shape measurements (coefficient of bias and kurtosis coefficient). Subsequently, normality tests are performed and, if necessary, a data transformation. In the AEDE, the application of regionalized variables is essential. It means that variables are distributed in space so that they present a spatial correlation structure.

## III. Results and Discussion

### *A. Geostatistical Data Analysis*

*1) Cu Statistical Measurements:* The distribution of Cu in the studied area is mostly uniform, with values that fluctuate between 4 and 80 ppm, except for the southeast part, where the concentration shoots up to 253 ppm. Figure 2 shows that the highest concentration of data is found in the first frequency, in the range of 3,900 to 29 ppm with a cumulative frequency of approximately 84%, concluding that the concentrations are in this range. Statistical measurements could be found in Table 1. With these statistical measures, the normality of the data is verified. The median and mean have similar values, but the mode has a different value. The coefficient of bias is greater than 1, so the curve has positive asymmetry, and the coefficient of variation is 84.93, which indicates that the effects caused by extreme values are tolerable. With these considerations, the copper concentration data must be subjected to a logarithmic transformation.

*2) Cu, Hg, As, Cu, and Zn Statistical Measurements:* The histograms are performed with each element's measured ppm. The statistical measurements of these elements are found in Table 1. In all histograms, except for zinc, the highest concentration of data is located in the first classes, suggesting its geochemical background.

TABLE I
Cu, Hg, As, Pb, and Zn Statistical Measurements (ppm)

| Parameter | Hg | As | Pb | Zn | Cu |
|---|---|---|---|---|---|
| | ppm | | | | |
| Minimum value | 0.100 | 2.800 | 5.500 | 5.600 | 4.470 |
| Maximum value | 1.310 | 80.240 | 401.000 | 212.700 | 253.200 |
| Average value | 0.140 | 6.800 | 27.470 | 56.310 | 22.640 |
| Median | 0.120 | 4.410 | 20.760 | 53.220 | 22.640 |
| Estándar desviation | 0.140 | 7.220 | 34.270 | 25.650 | 19.227 |
| Variance | 0.020 | 52.060 | 1174.570 | 657.670 | 369.680 |
| Coefficient of variation (%) | 94.900 | 106.170 | 124.780 | 45.540 | 84.930 |
| Statical bias | 6.130 | 5.610 | 7.950 | 1.710 | 8.140 |
| Kurtosis coefficients | 45.280 | 51.580 | 78.110 | 10.100 | 94.300 |
| 1 quartile | 0.110 | 2.800 | 15.530 | 41.850 | 14.530 |
| 3 quartiles | 0.140 | 8.380 | 29.520 | 67.770 | 26.010 |

With the statistical measurements obtained from the elements, the normality of the data is verified. For mercury, the mean, median, and mode values are not similar. The bias is 6.13, which indicates a positive asymmetry. The coefficient of variation is 94.90, which means that the effects caused by extreme values are tolerable. For the Cu. the normality of the data is verified. The median and mean have similar values, but the mode differs. The coefficient of bias is greater than 1. so the curve has positive asymmetry. The coefficient of variation is 84.93, which indicates that the effects caused by extreme values are tolerable.

In the case of arsenic, the mean, median, and mode are not similar. The bias is 5.61, which indicates a positive asymmetry. The coefficient of variation is 106.17. and it represents that the effects caused by extreme values are tolerable. For lead, the mean, median, and mode values are not similar. The bias is 7.95, which indicates a positive asymmetry, and the coefficient of variation is 124.78. It

means that the effects caused by extreme values are tolerable. For zinc, the mean, median, and mode values are not similar. The bias is 7.71, which indicates a positive asymmetry, and the coefficient of variation is 45.54. It also shows that the effects caused by extreme values are tolerable. Due to the above, the data of all the elements must be subjected to a logarithmic transformation. The statistical measurements of the transformed data for all the elements are summarized in Table 2.

For arsenic, the mean, median, and mode are similar. The bias is 0.93, which indicates a slight positive asymmetry, whereas the coefficient of variation is 40.75. It also represents that the effects caused by extreme values are tolerable. In the case of mercury, the mean, median, and mode are similar too. The bias is 3.05, which indicates a slight positive asymmetry, and the coefficient of variation is 154.09; although the value is relatively high, the effects caused by extreme values are tolerable. In the case of lead, the mean, median, and mode are similar. The bias is 1.26, which indicates a slight positive asymmetry, and the coefficient of variation is 18.13 what it means that the effects caused by extreme values are tolerable. For zinc, the mean, median, and mode are similar. The bias is -0.88, which indicates a slight negative asymmetry, and the coefficient of variation is 12.19. These are the effects caused by extreme values, and they are tolerable. In all cases, the bias improves markedly with the logarithmic transformation, and the normality of the curves is verified.

For the copper data previously transformed to logarithm, its normality is evidenced, and it is concluded that the mean, median, and mode have similar values. The bias coefficient is 0.500. and the coefficient of variation is 14.14. Due to this, the extreme data does not have much influence. So, the distribution is considered normal.

TABLE III
CU. HG. AS. PB. AND ZN STATISTICAL MEASUREMENTS (LOG)

| Parameter | Hg | As | Pb | Zn | Cu |
|---|---|---|---|---|---|
| | | | log | | |
| Minimum value | -1.000 | 0.450 | 0.740 | 0.750 | 0.650 |
| Maximum value | 0.120 | 1.900 | 2.600 | 2.330 | 2.400 |
| Average value | 0.120 | 0.710 | 1.340 | 1.710 | 1.290 |
| Median | -0.950 | 0.520 | 1.210 | 1.780 | 1.290 |
| Estándar desviation | 0.180 | 0.290 | 0.240 | 0.210 | 0.220 |
| Variance | 0.030 | 0.080 | 0.060 | 0.040 | 0.051 |
| Coefficient of variation (%) | 154.090 | 40.750 | 18.130 | 12.190 | 17.140 |
| Statical bias | 3.050 | 0.930 | 1.260 | -0.880 | 0.500 |
| Kurtosis coefficient s | 14.240 | 3.370 | 7.700 | 5.460 | 5.740 |
| 1 quartile | -1.000 | 0.450 | 1.190 | 1.620 | 1.160 |
| 3 quartiles | -0.860 | 0.920 | 1.470 | 1.830 | 1.420 |

Hg- GAUSSIAN MODEL

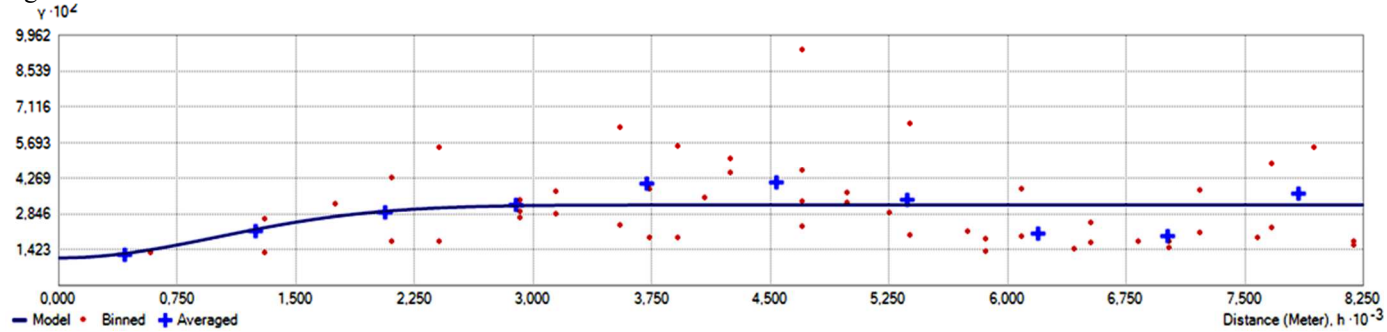


As- GAUSSIAN MODEL

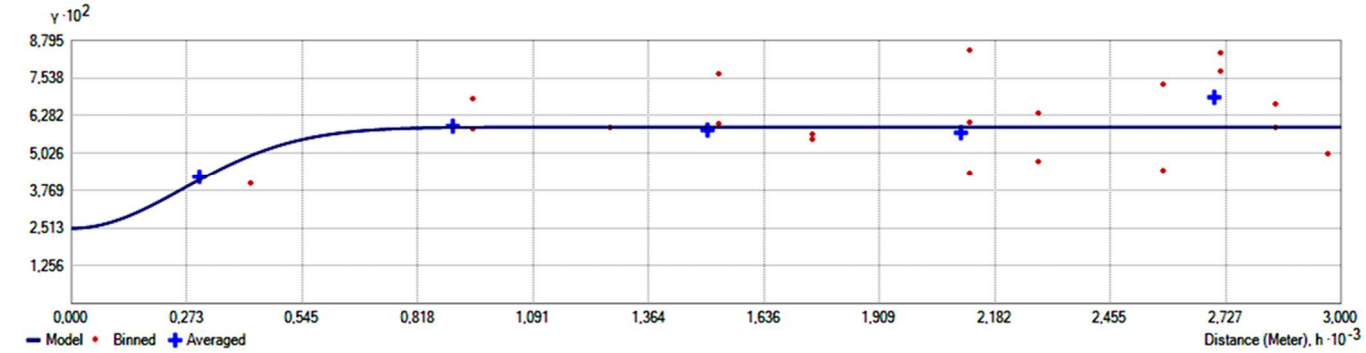

Zn-GAUSSIAN MODEL

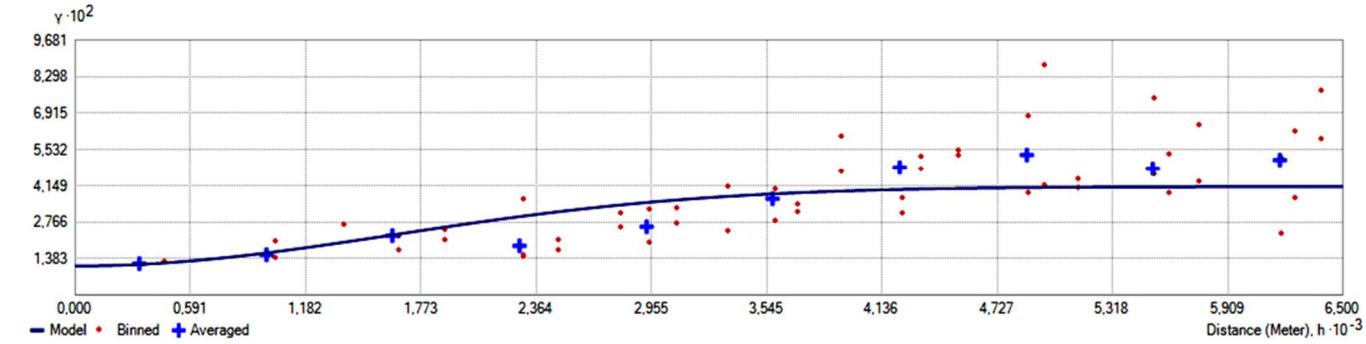


Pb- SPHERICAL MODEL

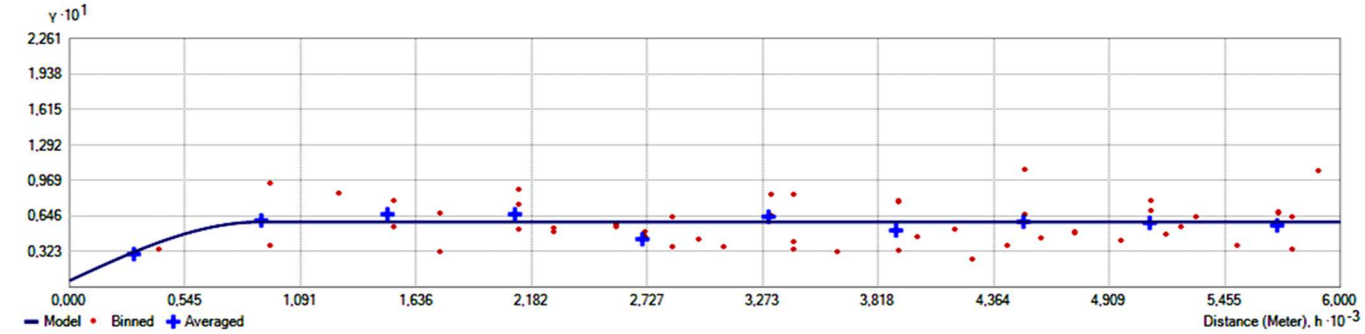


Cu- GAUSSIAN MODEL

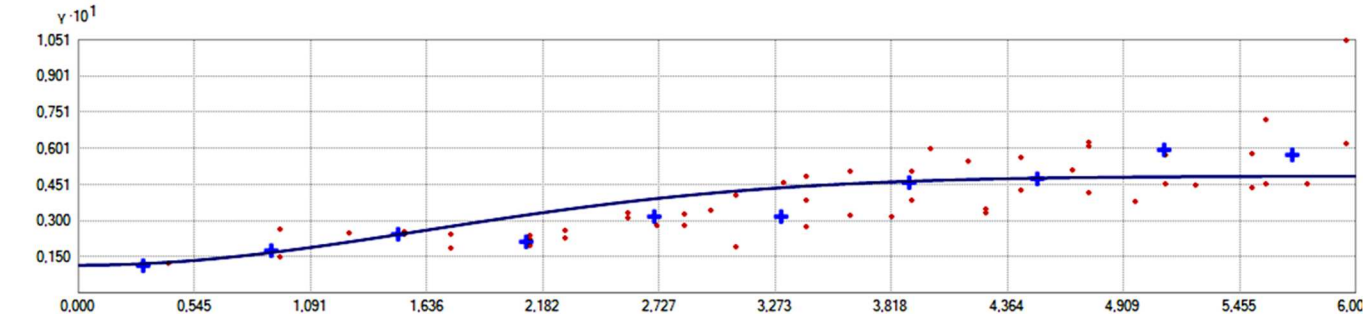


Fig. 2 Experimental semi variogram adjusted to the elements: Cu. Hg. As. Zn. Pb

*3) Geostatistics Theoretical Model:* Theoretical models were compared, spherical and Gaussian, to choose the best fit for the data and the one that generates the least error. Figure 2 shows the chosen models to this end. For elements like Hg, As, Cu, and Zn, the optimal model was the Gaussian, while Pb is the spherical model.

In the experimental semi variograms indicated with blue crosses in Figure 2. The semi variogram growth is observed according to the increases in the sampling distance to ranges ranging from 650 to 4.000 depends on the element analyzed. The theoretical model is indicated with a blue line. All the semi variograms have been brought as close as possible to the experimental one. Data that is not included in the range is considered random.

TABLE IIIII
MODEL PARAMETERS FOR ELEMENTS: HG. AU. AG. AS. SB. ZN. PB. CR. W

| Element | Model | Partial Sill | Nugget | Plateau | Variance | Lag Size | Angle | Range |
|---|---|---|---|---|---|---|---|---|
| Hg | Gaussian | 0.021 | 0.011 | 0.032 | 0.0324 | 825 | 47 | 2.450 |
| As | Gaussian | 0.034 | 0.025 | 0.059 | 0.0844 | 600 | 44 | 650 |
| Zn | Gaussian | 0.030 | 0.011 | 0.041 | 0.0435 | 650 | 3 | 4.000 |
| Pb | Spherical | 0.053 | 0.006 | 0.059 | 0.0594 | 600 | 15 | 900 |

As Table 3 shows, the sum of the nugget and partial sill does not exceed the variance in all cases. Also, the nugget is less than the partial sill, and it does not exceed 50% of the variance value, which shows no greater errors in data collection, processing, and chemical analysis. The angles and ranges are variable, and it shows that each phenomenon is independent with different characteristics [19].

– Hg

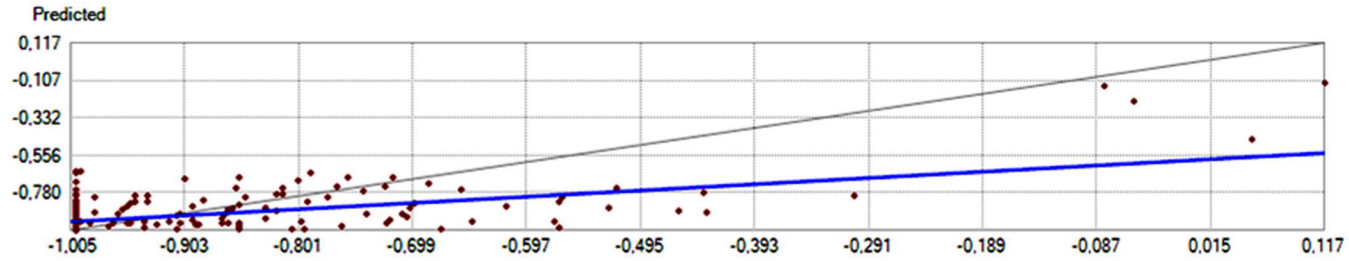


– As

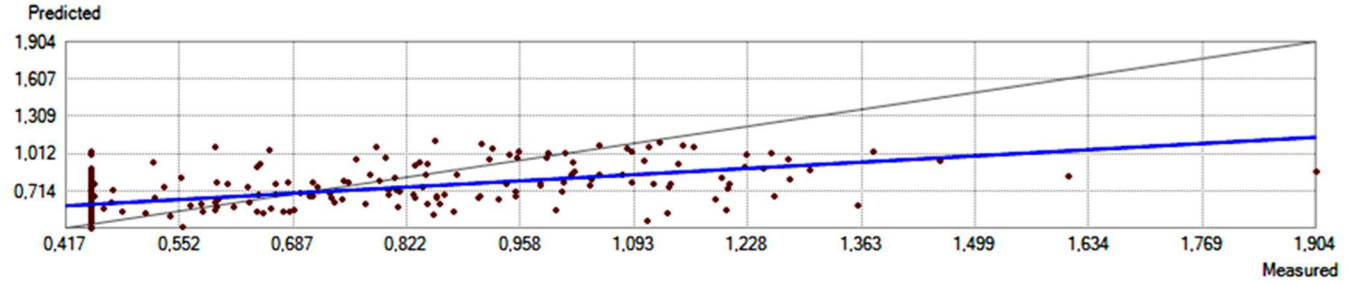


– Zn

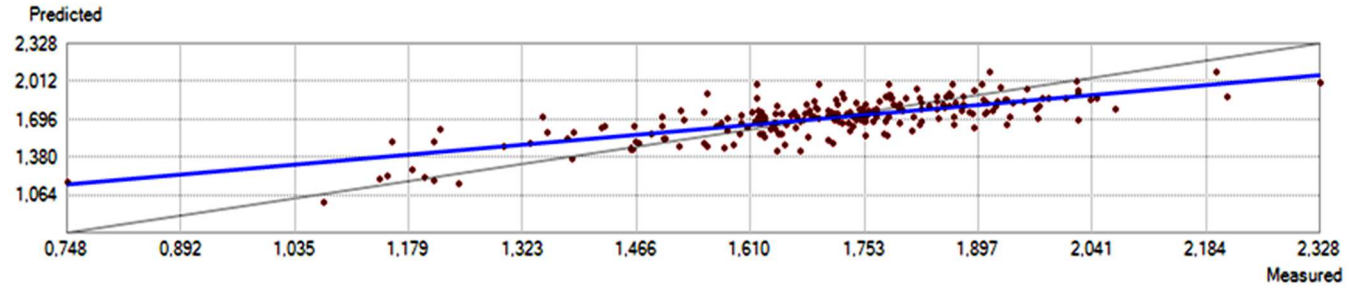


– Pb

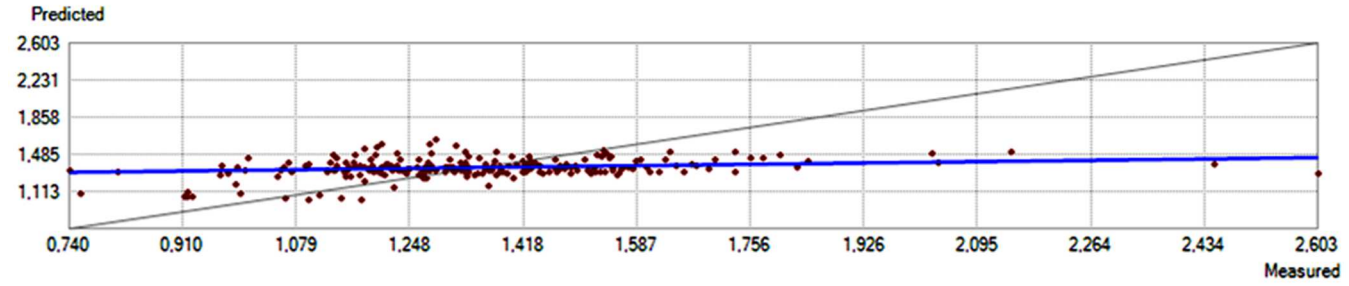


– Cu

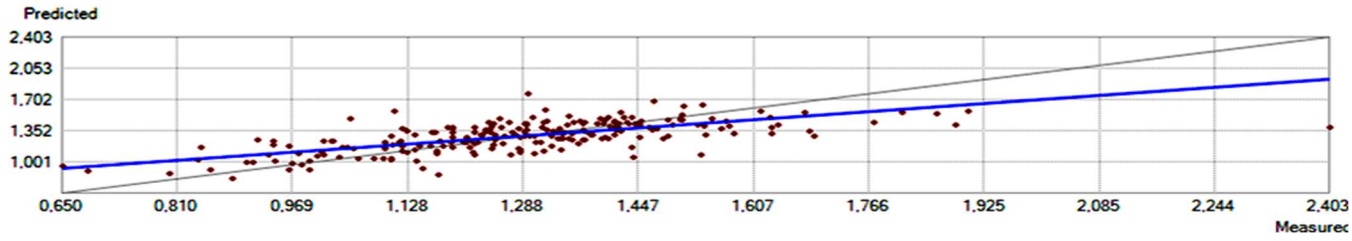


Fig. 3. Cross-validation of Cu. Hg. As. Zn. and Pb.

*4) Kriging Validation:* The kriging method is used to interpolate and predict values for unmeasured locations. giving weights to the surrounding measured values [16] [20-21]. This method helps spatially dependent variables and allows getting a linear unbiased estimation [22]-[23]. Figure 4 shows that there are prediction errors since the compared curves have a slight variation in the slope. However, they are considered acceptable because the standardized mean error and mean squared error values are close to 0 and 1, respectively. Table IV summarizes the parameters of the cross-validation of the elements: Cu, Hg, As, Zn, and Pb. The interpolation is considered valid in all the cases because the standardized mean error and the mean squared error are close to 0 and 1. compared to the other models (Gaussian and spherical).

TABLE IVV
CROSS-VALIDATION PARAMETERS OF THE ELEMENTS: CU. HG. AS. PB AND ZN

| Element | Model | Regression equation | Average square error | Standardized average error | Standardized average square Error |
|---|---|---|---|---|---|
| Hg | Gaussian | 0.3673 x -0.5855 | 0.13241 | 0.13744 | 0.96582 |
| As | Gaussian | 0.3678 x +0.4411 | 0.24976 | 0.25262 | 0.98874 |
| Zn | Gaussian | 0.5775 x +0.7195 | 0.13435 | 0.12873 | 1.05598 |
| Cu | Gaussian | 0.5722 x + 0.5555 | 0.16871 | 0.13237 | 1.23796 |
| Pb | Spherical | 0.0789 x +1.2479 | 0.23185 | 0.25262 | 0.91798 |

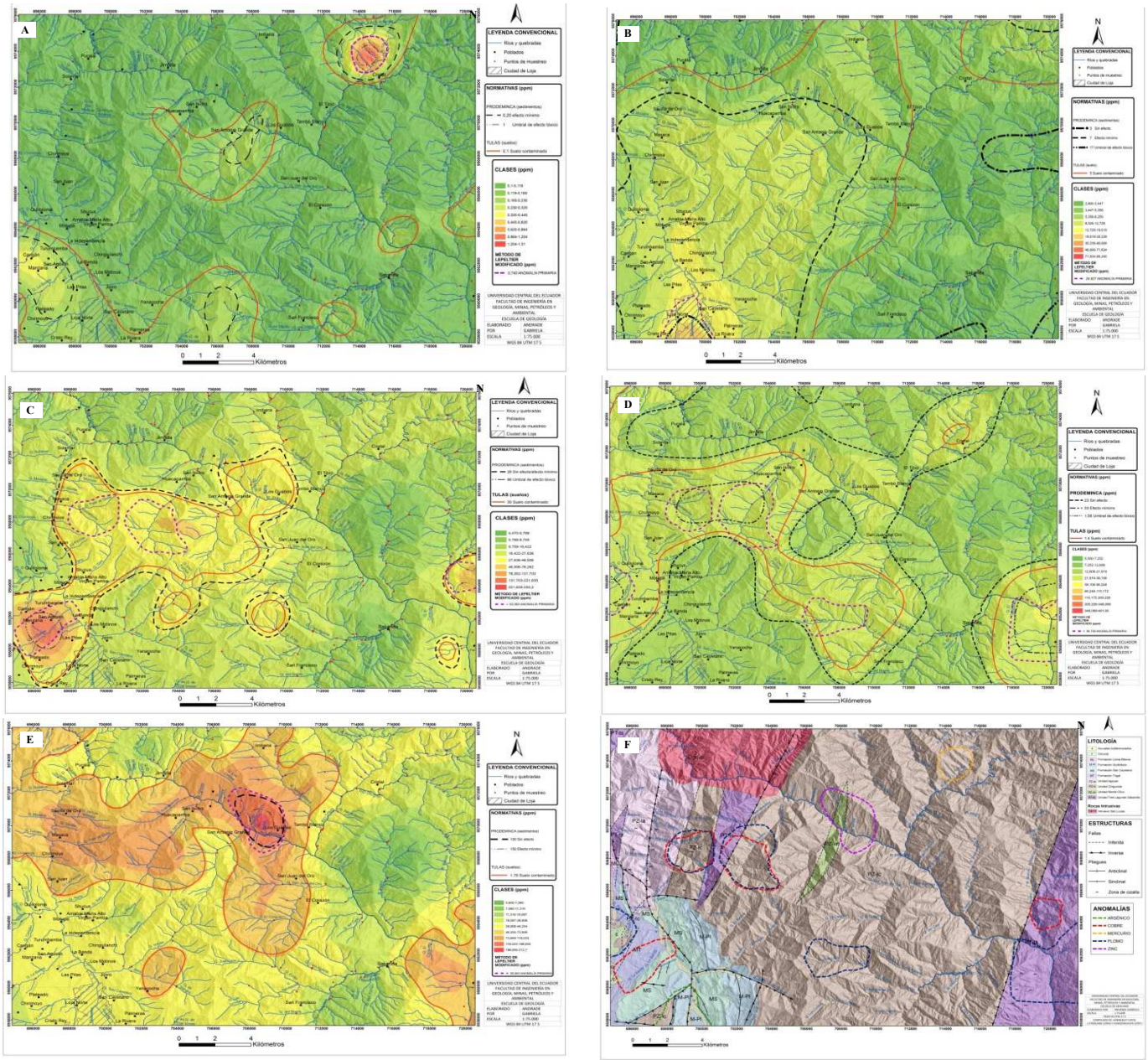


Fig. 4 Spatial distribution of anomalies: A: Hg. B: As. C: Cu. D: Pb. E: Zn. F: Anomalies and geology correlation

*5) Spatial Distribution Maps:*

- Mercury

To the NW of the studied sector, a defined anomaly is observed in the sector of the Río Tibio with samples from four tributary streams affecting the Cristal town. Sub anomalies in other streams, such as Los Lumos, La Banda, and Onda, exceed the environmental regulations, but since they do not present anthropic risk activities. They are related to the background (figure 4-A). It is not recommended to carry out fish farming activities or consume the raw water in both cases. This anomaly could be related to the artisanal mining activities that the inhabitants reported. However, when not

verified, it could also be associated with mineralization since mercury's main sources are natural [24].

The values are exceeding the norm by a considerable value, and it could cause damage to human health since in this town the main food is "trout" type fish. This type of fish could easily bio-accumulate the metal as well other species of ingested vegetables [25].

The main anomaly cannot be associated with the Metallogenic Map (1980), where the indication is in the Zamora-Huayco river's vicinity. It runs in the opposite direction to the location of the main anomaly and is approximately 30 km away. However, secondary anomalies may be associated with the indication is they are proximal. they are related to deposits in the sedimentary basin Loja (figure 4-F).

- Arsenic

In figure 4-B, a defined anomaly is observed in Loja, which has a high percentage of uncertainty since being on edge, the software can present interpolation errors. However, along the Zamora Huayco river to Sevilla de Oro, a subnormal is observed that must be taken into account because it is of great extension (approximately 32 $km^2$). Values exceed the norm, and many villages are found. Consumption of untreated water is not recommended; even skin contact should be avoided that is vital for the city of Loja because it has a high number of inhabitants.

There are no mining activities with which arsenic can be associated. So, these anomalies can be related to sulfide mineralization such as arsenopyrite present in the sector. It would be advisable to find the source since the sub anomaly is highly widespread. This anomaly can also be related to industrial emissions, agriculture, municipal waste disposal, and domestic discharges since it is located in an urban area [26]. In other surveys was concluded that fertilizers, the discharge of wastewater, and the accumulation of garbage are causes of contamination at Loja City [27].

- Copper

Figure 4-C is possible to observe the main anomaly near the Loja city in the La Banda stream and two sub anomalies in the Mamanuma and San Isidro streams. The values of the anomaly and sub anomalies exceed the regulations (TULAS) and in international regulations, it is considered as a threshold of toxic effect. It has considerable uncertainty because it is located on the western edge of the study area. Other sectors exceed the regulations, but the values are associated with the background. Great care must be taken to consume aquatic life and plants that accumulate the metal [28]. In addition, it can produce a decrease in the properties of the soil when used for agriculture [29]. In the case of sub anomalies, they are associated with sulfides ince the specific sectors. The main anomaly is associated with the Metallogenic Map's indication, which mentions mineralization of metasomatic origin in metamorphic rocks, particularly from weathering, and might be transferred by colloid mineral particulates [30].

- Lead

In figure 4-D, the main anomaly is observed in a range of 90.709 to 476.636 ppm towards the SE, which has considerable uncertainty. However, the secondary one is highly reliable and coincides with international regulations, but this is considered minimal.

There are secondary anomalies in a range of 30.012 to 90.709 ppm in the Carigán gorge, in the Mamanuma, and San Isidro gorge. The third is in the Zurita gorge, and the last in the source of the Blanco River. All present sampled values exceed national regulations, including in sub anomaly areas. With this element, great care must be taken in the food that is consumed, especially in some vegetables since they bioaccumulate [29]. In this sense, it is necessary to consider toxic metal remediation because hazardous heavy metals can enter the food chain and bio magnify due to contaminated product consumption [31]-[33]. The sub anomalies are associated with indications from the Metallogenic Map (Paladins 1980) linked to the location of the San Lucas intrusive and could also be associated with local polysulfide mineralization.

- Zinc

As can be seen in figure 4-E, this element presents a defined primary anomaly that even coincides with international regulations. It occurs in the Alvear and Onda stream, with defined values taken in each of them that are in the range of 95.940 to 245.092 ppm. There are also secondary anomalies whose lower range value coincides with national regulations. They are in the range of 60.026 to 95.940 ppm; indicating that the entire sector is at potential risk. Great care must be taken to consume foods that bioaccumulate zinc and in soils with high values since their properties for agricultural use are reduced.

The sub anomalies of this element are associated with indications from the Metallogenic Map (Paladins 1980) linked to the San Lucas intrusive location. The main defect of zinc and minor anomalies could also relate to local sulfide mineralization and the presence of tectonic flake Mount Olive Formation (figure 4-F). A significant correlation was observed between Pb and Cu at San Isidro and Masaca ravines, indicating that they were from the same origin [19]. associated with local polysulfide mineralization.

## IV. Conclusion

Three types of lithology predominate in the study area: the metamorphic units (Sabanilla, Tres Lagunas, Chigüinda, Monte Olivo, Agoyán). The sediments of the Loja basin (Trigal, San Cayetano, Loma Blanca, and Quillollaco), and the intrusive of San Lucas. The lack of background values in the micro-basins that drain through areas with mineral anomalies prevents a geological/metallogeny baseline from being adjusted to reality [29]. To solve this constraint. The application of the Lepeltier method to determine the concentrations of metallic elements and their potential impact on ecosystems is viable. To be specific, the Lepeltier method works on a lognormal element concentration distribution, takes measured data, and processes it by removing atypical values to get a normal distribution [34]. The rural towns affected by the high concentrations of Cu are Masaca, Chirimoyo, Huacapamba, and Manzana.

National regulations (TULAS) for soils and international regulations (Environment Canada) for river sediments have been used in this context. In the area under study, there is no formal metallic mining activity now. So, the anomalous concentrations of metallic elements are characteristic of the lithology. As a result, remediation programs are not required.

But near Loja City, it is advisable to make a holistic environmental assessment to estimate the environment's health [35]. This research can also be used as an environmental baseline for future mining projects in the sector.

## ACKNOWLEDGMENT

The authors are grateful to the IIGE for its help in preparing this document and Universidad International SEK for its cooperation and the whole research.

## REFERENCES

[1] Trouw. R. Cuatro cortes por la faja metamórfica de la Cordillera Real. Ecuador. Guayaquil- Ecuador: Escuela Politécnica del Litoral.. 1976.

[2] Litherland. M.. J. A. Aspden. y R. A. Jemielita. The Metamorphic Belts of Ecuador: Overseas Memoir of the British Geological Survey. Keyworth. 1994.

[3] Jemielita. R. y Bolaños. J. Mineralización. potencial mineral y metalogénesis de la Cordillera Real del Ecuador. Quito-Ecuador: CODIGEM Misión Británica. 1993.

[4] Izquierdo. O. «Estudio Geodinámico de la Cuenca Intrammontañosa cenozoica de Loja (Sur del Ecuador). Tesis de ingeniería no publicada.» Quito. Ecuador. 1991.

[5] Hungerbühler. D.. Steinmann. M.. Winkler. W.. Seward. D.. Egüez. A.. Peterson. D.. Helg.U. y Hammer. C. Neogene Stratigraphy and Andean geodynamics of southern Ecuador.Earth-Science Reviews. p. 75-124. 2002.

[6] Correa. C. «Análisis de la susceptibilidad de los fenómenos de remoción en masa de la carretera Loja-Zamora.» Tesis de Grado. Facultad de Geología y Petróleos. Escuela Politécnica Nacional. Quito. Ecuador. 2007.

[7] Zhao. G. et al.. Distribution and contamination of heavy metals in surface sediments of the Daya Bay and adjacent shelf. China. Marine Pollution Bulletin (2016)

[8] Ahmad. K. et al.. Occurrence. source identification and potential risj evaluation of heavy metals in sediments of the Hunza River and its tributaries. Gilgit-Baltistan. Environmental Technology & Innovation 18 (2020)

[9] Lin. X. et al.. Geochemical patterns of Cu. Au. Pb and Zn in stream sediments from Tongling of East China: Compositional and geostatistical insights. Journal of Geochemial Exploration 210 (2020)

[10] Amrit Kumar. et al.. Mapping spatial distribution of traffic induced criteria pollutants and associated health risks using kriging interpolation tool in Delhi. Journal of Transport & Health. 18 (2020). doi.org/10.1016/j.jth.2020.100879.

[11] Shafie. N. et al.. Geoaccumulation and distribution of heavy metals in the urban river sediment. International Journal of Sediment Research. Vol. 29. N°. 3 (2014)

[12] Sanjoy Shil. and Umesh Kumar Singh. Health risk assessment and spatial variations of dissolved heavy metals and metalloids in a tropical river basin system. Ecological Indicators. 106 (2019). doi.org/10.1016/j.ecolind.2019.105

[13] Kyeonghwan Kang. et al.. Modified screening-based Kriging method with cross validation and application to engineering design. Applied Mathematical Modelling. 70 (2019). doi.org/10.1016/j.apm.2019.01.030.

[14] Mahyadin Mohammadpour. et al.. Geochemical distribution mapping by combining number-size multifractal model and multiple indicator kriging. Journal of Geochemical Exploration. 200 (2019). doi.org/10.1016/j.gexplo.2019.01.018.

[15] Gia Pham. T.; et al.. Application of Ordinary Kriging and Regression Kriging Method for Soil Properties Mapping in Hilly Region of Central Vietnam. Geo-Information. 147 (2019). doi.org/10.3390/ijgi8030147

[16] Yarahmadi. S.. Ansari. M.. Ecological risk assessment of heavy metals (Zn. Cr. Pb. As and Cu) in sediments of Dohezar River. North of Iran. Tonekabon city. Acta Ecologica Sinica (2016)

[17] Sandeep Kumar. et al.. Hazardous heavy metals contamination of vegetables and food chain: Role of sustainable remediation approaches - A review. Environmental Research. 179 (2019). doi.org/10.1016/j.envres.2019.108792.

[18] El-Sorogy. A. et al.. Distribution. source. contamination. and ecological risk status of heavy metals in the Red Sea-Gulf of Aqaba coastal sediements. Saudi Arabia. Marine Pollution Bulletin 158 (2020)

[19] Tahril. T.. et al.. Profile of metals Fe in lay ecosystem using ICP-OES in Donggala District. Indonesia. Current Chemistry Letters. 9 (2020). 10.5267/j.ccl.2019.11.001

[20] Nakić. Z. et al.. Ambient Background Values of Selected Chemical Substances in Four Groundwater Bodies in the Pannonian Region of Croatia. Water. 12 (2020). doi.org/10.3390/w12102671

[21] TULAS. «Texto unificado de legislación ambiental.» Quito. Ecuador. 2007.

[22] Yang. P. G.. Mao. R.. Shao. H.. Gao. Y. The spatial variability of heavy metal distribution in the suburban farmland of Taihang Piedmont Plain. China. C.R. Biologies 332 (2009)

[23] Sahoo. P.K. et al.. Regional-scale mapping for determining geochemical background values in souls of the Itacaiúnas River Basin. Brazil: The use of compositional data analysis. Geoderma 376 (2020)

[24] Kabata-Pendias. A. Soil-plant transfe of trace elements- an environmental issue. Geoderma 122 (2004)

[25] Cuculic. V. et al.. Natural and anthropogenic sources of Hg. Cd. P. Cu and Zn in seawater and sediment of Mljet National Park. Croatia. Estuarine. Coastal and Shelf Science 81 (2009)

[26] Kabata-Pendias. A.. Pendias. H. Trace Elements in Soils and Plants. 3rd ed. CRC Press. Boca Ratón. Fl. (2001)

[27] Akomaye. A.. & Unimuyi. U.. Concentration of Heavy Metals (Cd. Co. Cr. & Fe) in Soil and Edible Vegetables in Obudu Urban Area of Cross River State. Nigeria. Chemical Science International Journal. 27 (20191). doi.org/10.9734/CSJI/2019/v27i130105

[28] Awe. A. et al.. Occurrence and probabilistic risk assessment of PAHs in water and sediment samples of the Diep River. South Africa. Heliyon 6 (2020)

[29] Ruiz-Pico. A. et al.. Hydrochemical characterization of groundwater in the Loja Basin (Ecuador). Applied Geochemistry 104 (2019) 1–9

[30] Lorenzo Morroni. et al.. Integrated characterization and risk management of marine sediments: The case study of the industrialized Bagnoli area (Naples. Italy). Marine Environmental Research. 160 (2020). doi.org/10.1016/j.marenvres.2020.104984.

[31] Shunan Zheng. et al. Human health risk assessment of heavy metals in soil and food crops in the Pearl River Delta urban agglomeration of China. Food Chemistry. 316 (2020). doi.org/10.1016/j.foodchem.2020.126213.

[32] Yuezhao Li. et al.. Source apportionment and source-oriented risk assessment of heavy metals in the sediments of an urban river-lake system. Science of The Total Environment. 737 (2020). doi.org/10.1016/j.scitotenv.2020.140310.

[33] Rostami. A.A.. et al. Evaluation of geostatistical techniques and their hybrid in modelling of groundwater quality index in the Marand Plain in Iran. Environ Sci Pollut Res 26. 34993–35009 (2019). doi.org/10.1007/s11356-019-06591-z

[34] Linnik. V.G. et al. Spatial distribution of heavy metals in soils of the flood plain of the Seversky Donets River (Russia) based on geostatistical methods. Environ Geochem Health (2020). doi.org/10.1007/s10653-020-00688-y

[35] Zakir. H. M.. et al.. Health Risk Assessment of Heavy Metal Intake of Common Fishes Available in the Brahmaputra River of Bangladesh. Archives of Current Research International. 19 (2019). doi.org/10.9734/acri/2019/v19i230153